Research Square

Preprints are preliminary reports that have not undergone peer review.
They should not be considered conclusive, used to inform clinical practice,
or referenced by the media as validated information.

Hot-Water Extraction and Multi-Stage Refining of Tobacco Stems Balance Bulkiness and Strength in Reconstituted Tobacco Sheets

Qianqian Zhao
South China University of Technology
Mengting Ye
South China University of Technology
Huilin Hu
South China University of Technology
Xinke Yuan
Technology Center of Hunan Tobacco Industry Co., Ltd.
Jun Li
ppjunli@scut.edu.cn
South China University of Technology

Research Article

Keywords: Tobacco stem, Hot-water extraction, Multi-stage refining, Fiber morphology, Reconstituted tobacco sheet

Posted Date: November 9th, 2026

DOI: https://doi.org/10.21203/rs.3.rs-10410154/v1

License: This work is licensed under a Creative Commons Attribution 4.0 International License.
Read Full License

Additional Declarations: No competing interests reported.

Abstract

Balancing bulkiness and mechanical strength is critical for preparing high-quality reconstituted tobacco sheets from tobacco stem fibers. Herein, mild hot-water extraction combined with multi-stage refining was used to regulate fiber morphology and porous network structure. Micro-CT showed that hot-water extraction loosened the compact internal structure of tobacco stems, facilitating fiber separation and fibrillation during refining. As the refining pass increased, the beating degree increased from 22 °SR to 31 °SR, and the fine pulp yield increased from 5.33% to 12.23%. Two-stage refining produced the most favorable fiber morphology, with sufficient fibrillation and limited fiber damage. Consequently, the tensile strength and elongation reached maximum values of 0.371 $kN \cdot m^{-1}$ and 1.030% at 28 °SR, while maintaining a relatively high bulk of 11.560 $cm^3 \cdot g^{-1}$. Further refining compacted the fiber network and reduced bulk to 10.155 $cm^3 \cdot g^{-1}$. SEM and micro-CT analyses confirmed that moderate refining formed a uniform and interconnected porous network, enabling an improved bulkiness-strength balance. These findings clarify how controlled fiber fibrillation and pore-network regulation jointly govern the bulkiness-strength balance of reconstituted tobacco sheets.

Highlights

1. Mild hot-water extraction loosened the compact structure of tobacco stems.
2. Multi-stage refining regulated fiber morphology and fine pulp formation.
3. Two-stage refining at 28 °SR achieved the best bulkiness–strength balance.
4. Micro-CT revealed pore-network evolution during tobacco stem refining.
5. Controlled fibrillation enabled stronger yet still bulky cellulose-rich sheets.

Introduction

Tobacco stems are major lignocellulosic by-products generated during tobacco processing and represent an important fiber source for reconstituted tobacco sheets (Chaowei et al. 2019; Shakhes et al. 2023; Berhanu Lemma et al. 2024; He et al. 2025). The conversion of tobacco stems into sheet materials not only improves the utilization efficiency of tobacco residues, but also provides a practical route for producing uniform tobacco-based sheets with controlled physical properties (Hu et al. 2025). Among these properties, bulkiness and mechanical strength are particularly important. High bulkiness benefits filling capacity, liquid absorption and air permeability, whereas sufficient tensile strength is required for subsequent coating, drying, cutting and converting processes (Chaowei et al. 2019; Song et al. 2021; Huang et al. 2024; Liu et al. 2024). However, these two properties are often contradictory in fiber-based porous sheets: loose networks favor high bulkiness, while dense and well-bonded networks usually provide higher strength (Huang et al. 2024).

Fiber morphology regulation is essential for resolving this bulkiness-strength trade-off. During refining, tobacco stem fibers undergo swelling, separation, fibrillation, deformation and partial shortening (Zhao

et al. 2018; Huang et al. 2024). Moderate refining can expose fibrils, increase inter-fiber bonding area and enhance stress transfer within the sheet network. In contrast, insufficient refining leads to poor fiber dispersion and weak bonding, while excessive refining may generate excessive fine components, compact the porous network and reduce bulkiness (Bajpai 2018; Ang et al. 2019; Berhanu Lemma et al. 2024). Therefore, the key is not simply to increase refining intensity, but to control fiber fibrillation and network structure within an appropriate range (Berhanu Lemma et al. 2024; Li et al. 2026).

Pretreatment before refining is an important strategy for improving the processability of lignocellulosic fibers. Compared with chemical or enzymatic pretreatments, hot-water extraction is mild, simple and compatible with the conventional preparation process of reconstituted tobacco sheets (Leszczyński and Roman 2023; Hu et al. 2024; Li et al. 2024; Liu et al. 2026). In tobacco sheet production, extraction is usually regarded as a step for separating soluble constituents from solid residues, while its potential influence on subsequent fiber refining and sheet formation has received less attention (Luo et al. 2021; Puițel et al. 2023). In particular, the relationship among hot-water extraction, multi-stage refining, fiber morphological evolution and the final bulkiness-strength balance of tobacco stem-based sheets remains insufficiently understood.

Herein, mild hot-water extraction combined with multi-stage refining was used to regulate tobacco stem fibers and prepare reconstituted tobacco sheets with balanced bulkiness and strength (Fig. 1). The internal structure of tobacco stems before and after hot-water extraction was compared by micro-CT (Li et al. 2021; Dallé et al. 2021; Li et al. 2023; Tao et al. 2025). The morphological evolution of coarse and fine pulp fractions during refining was systematically analyzed, including fiber length, width, coarseness, aspect ratio, curl index, kink index, fibrillation degree and broken fiber ratio. The effects of refining pass on beating degree, fine pulp yield, tensile strength, elongation and bulk were further evaluated. SEM and micro-CT were used to reveal the microstructural and pore-network evolution of tobacco stem-based sheets (Dallé et al. 2021), aiming to clarify how pretreatment-assisted refining regulates fiber morphology, porous structure and sheet performance (Sharma et al. 2015; Hayase et al. 2021).

Methods and Experiments

Materials

Tobacco stems were obtained from a local cigarette factory. The stems were air-dried and sealed in bags for storage prior to use.

Preparation of Reconstituted Tobacco Sheets

Hot-water extraction pretreatment

The dried tobacco stems were mixed with deionized water at a solid-to-liquid ratio of 1:10 (based on oven-dry weight) and extracted at 80°C for 30 min to remove soluble components and loosen the tissue

structure. After extraction, the stems were drained and a portion was freeze-dried for subsequent structural observation.

Refining and screening

The pretreated stems were refined using a laboratory-scale refining system (self-built) for one, two, or three passes to obtain pulps with different refining intensities. The refined pulps were then screened with a flat screen to separate coarse and fine fractions. The fine pulp yield was calculated as the percentage of oven-dry fine pulp relative to the total oven-dry raw material. The beating degree of each pulp fraction was determined using a beating degree tester according to standard methods.

Sheet forming and drying

Handsheets with a target basis weight of 60 g·m^{-2} were prepared from the fine pulp fractions obtained after each refining pass using a laboratory sheet former. The wet sheets were freeze-dried at -60°C for 24 h to preserve the original porous structure. The dried sheets were conditioned at (23 ± 1) °C and (50 ± 2)% relative humidity for 24 h prior to testing.

Characterization

Fiber morphology analysis

Fiber morphological parameters, including length-weighted average fiber length, width, coarseness, curl index, kink index, fibrillation degree, and broken fiber ratio, were measured for both coarse and fine pulp fractions using a MorFi fiber analyzer (Techpap, France) (Sood and Sharma 2021). For each sample, at least 10,000 fibers were counted to ensure statistical reliability.

Physical property measurements

Tensile strength and elongation were tested using an L&W tensile strength tester (CE062, Sweden) with a clamping length of 100 mm and a crosshead speed of 20 mm·min^{-1}. Sheet thickness was measured with an L&W thickness tester (L251-5508, Sweden), and bulk was calculated as the ratio of thickness (cm^3) to basis weight (g), expressed in cm^3·g^{-1}.

Microstructural and pore structure characterization

The internal structure of tobacco stems before and after hot-water extraction, as well as the cross-sectional morphology of the sheets, was observed using scanning electron microscopy (SEM). Three-dimensional nondestructive scanning of the sheet samples was performed using a micro-computed tomography system (SkyScan 2211, Bruker, Germany) operated at 90 kV and 105 μA, with an exposure

time of 0.5 s, a pixel size of approximately 5 μm, and 1800 projections acquired over a 180° rotation. The image stacks were reconstructed with VoxelStudioRecon software, and three-dimensional models were built using Avizo software to extract pore structure parameters such as porosity and pore size distribution. A region of interest (ROI) of 800 × 400 × 800 voxels, verified as a representative volume element (RVE), was selected for the analysis (Sharma et al. 2015; Li et al. 2021; Wang et al. 2023).

Grey relational analysis

Grey relational analysis (GRA) was used to quantitatively evaluate the correlations between fiber morphological/structural parameters and sheet properties (Jamshaid et al. 2022; Samuel et al. 2022; Huo et al. 2023). The performance indices (tensile strength, elongation, and bulk) were taken as the reference sequences, and the fiber morphological or pore structural parameters as the comparison sequences. After mean-value normalization, the grey relational coefficients were calculated with a distinguishing coefficient ρ = 0.5 (Vujji and Dahiya 2023). The grey relational degrees were then ranked; a higher degree indicates a more significant influence.

Results and Discussion

Hot-water extraction loosens the compact structure of tobacco stems

The internal architecture of tobacco stems before and after hot-water extraction was visualized by micro-CT to clarify the structural basis for subsequent fiber disintegration and refining. As shown in Fig. 2a, the untreated tobacco stem displayed a compact and highly heterogeneous cross-sectional structure. The vascular bundles and surrounding parenchyma tissues were closely packed, and the internal voids were partially blocked by dense cell-wall materials and extractives. This compact structure limits water penetration and reduces the accessibility of mechanical forces during refining (Sung and Seo 2009; Hu et al. 2024; Liu et al. 2026). After hot-water extraction, the cross-section became more open and structurally distinguishable (Fig. 2b). The vascular tissue, cell lumens and porous regions were more clearly exposed, indicating that soluble compounds, weakly bound components and part of the amorphous matrix were removed during extraction (Sun et al. 2021). This structural loosening is beneficial for water penetration, fiber swelling and fiber separation during subsequent refining. Therefore, hot-water extraction acts not only as a conventional extraction step for removing water-soluble constituents, but also as a mild pretreatment that improves the mechanical processability of tobacco stem fibers (Li et al. 2025).

Morphological evolution of coarse and fine pulp fibers during multi-stage refining

The morphological evolution of tobacco stem fibers during multi-stage refining was analyzed by separately evaluating the coarse and fine pulp fractions. As shown in Fig. 3a–d, the coarse pulp

exhibited a pronounced response to refining. The average fiber length of the coarse pulp remained relatively stable after the first and second refining passes, increasing slightly from 0.433 mm to 0.438 mm, and then decreased to 0.417 mm after the third pass. In contrast, the fiber width decreased continuously from 31.84 μm to 28.16 μm and further to 23.63 μm with increasing refining pass. As a result, the calculated fiber aspect ratio increased from approximately 13.6 to 15.6 and 17.6. This indicates that multi-stage refining mainly promoted longitudinal splitting and fiber narrowing in the coarse fraction, rather than severe fiber shortening.

The fiber coarseness of the coarse pulp first decreased from 10.733 mg/m to 8.860 mg/m after the second refining pass, suggesting improved fiber separation and partial fibrillation. However, it increased sharply to 20.607 mg/m after the third pass, which may be related to the retention of relatively thick residual fiber fragments or aggregated coarse fiber components after excessive refining. Meanwhile, the curl index decreased continuously from 42.96% to 37.68% and 35.27%, indicating that the coarse fibers became straighter and more conformable during refining. The kink index changed only slightly, remaining around 14.5–15.3%, suggesting that refining altered fiber flexibility and surface structure more strongly than kink deformation. The fibrillation degree of the coarse pulp increased progressively from 10.660% to 13.494% and 14.274%, confirming that repeated refining enhanced external fibrillation and exposed more bonding sites on the fiber surface (Motamedian et al. 2019; Ushakov et al. 2023). Notably, the broken fiber ratio decreased from 41.842% to 39.822% and further to 31.703%. This result suggests that hot-water extraction followed by controlled refining favored fiber bundle opening and fibrillation rather than destructive cutting of the coarse fibers.

The fine pulp fraction showed a different morphological evolution pattern (Fig. 3e–h). The average fiber length increased from 0.370 mm to 0.391 mm after the second refining pass and then slightly decreased to 0.383 mm after the third pass. The fiber width increased from 28.50 μm to 29.43 μm and then remained close to 28.98 μm. Accordingly, the aspect ratio of the fine pulp changed only slightly, from approximately 13.0 to 13.3 and 13.2. These results indicate that the fine pulp fibers were less affected in terms of dimensional change compared with the coarse pulp fibers.

The coarseness of the fine pulp increased gradually from 12.700 mg/m to 13.563 mg/m and 13.955 mg/m with increasing refining pass. The curl index decreased from 43.70% to 41.43% after the second pass and then recovered to 42.96% after the third pass, while the kink index slightly increased from 15.20% to 15.40% and then decreased to 14.80%. More importantly, the fibrillation degree of the fine pulp increased from 20.816% to 23.340% after the second refining pass, indicating enhanced fiber surface development. After the third refining pass, it slightly decreased to 22.018%, suggesting that excessive refining did not further improve fine fiber fibrillation. The broken fiber ratio decreased markedly from 20.870% to 15.170% after the second pass, but increased again to 19.572% after the third pass. This confirms that two-stage refining was more favorable for producing fine pulp fibers with high fibrillation and low fiber damage.

Refining pass regulates pulp development and the bulk-strength balance of tobacco stem sheets

The effect of refining pass on pulp development and the physical properties of reconstituted tobacco sheets is shown in Fig. 4. As the refining pass increased from one to three, the beating degree increased from 22 °SR to 28 °SR and further to 31 °SR (Fig. 4a). Meanwhile, the fine pulp yield increased continuously from 5.33% to 8.40% and 12.23%, respectively. This result indicates that multi-stage refining progressively promotes fiber swelling, fibrillation and fiber bundle disintegration, producing more fine pulp components and improving the drainage resistance of the pulp suspension (Kunfong et al. 2023).

The tensile strength and elongation of the sheets exhibited a non-monotonic trend with increasing refining pass (Fig. 4b). The tensile strength increased from 0.335 $kN \cdot m^{-1}$ after one refining pass to 0.371 $kN \cdot m^{-1}$ after two refining passes, corresponding to an increase of approximately 10.7%. The elongation also increased from 0.918% to 1.030%. This improvement can be attributed to enhanced fiber fibrillation and increased inter-fiber bonding area, which improved stress transfer within the sheet network. However, after three refining passes, the tensile strength decreased to 0.353 $kN \cdot m^{-1}$ and the elongation decreased to 0.974%. Although the beating degree and fine pulp yield continued to increase, excessive refining did not further improve mechanical performance. This suggests that over-refining may partially damage fiber integrity, increase structural densification and weaken the contribution of the coarse fiber skeleton (Li et al. 2025).

In contrast, the bulk of tobacco stem sheets decreased continuously with increasing refining pass (Fig. 4c). The bulk decreased from 12.212 $cm^3 \cdot g^{-1}$ after one refining pass to 11.560 $cm^3 \cdot g^{-1}$ after two refining passes and further to 10.155 $cm^3 \cdot g^{-1}$ after three refining passes. The total decrease reached approximately 16.8% from the first to the third refining pass. This decline is consistent with the progressive collapse and densification of the fiber network during refining. At low refining intensity, the sheet retained a loose porous structure and therefore exhibited high bulk. With increasing refining intensity, fibrillated fibers and fine components filled the inter-fiber voids and enhanced fiber bonding, resulting in a denser network and lower bulk (Zhao et al. 2018).

The grey relational analysis further revealed the contribution of fiber morphological characteristics to sheet performance (Fig. 4d). Tensile strength showed the highest correlation with fibrillation degree, with a grey relational degree of 0.862, followed by cut fiber ratio and fiber length, with values of 0.827 and 0.795, respectively. This indicates that mechanical reinforcement is mainly governed by the development of fiber surface fibrillation and the preservation of sufficient fiber length. Bulk was most closely related to fiber coarseness, with a grey relational degree of 0.768, followed by fiber length and curl index, with values of 0.713 and 0.697, respectively. These results suggest that coarse and relatively long fibers are beneficial for constructing a loose and supportive fiber network. For elongation, curl index showed the highest correlation, with a grey relational degree of 0.815, followed by fiber length and fibrillation degree, with values of 0.764 and 0.742, respectively, indicating that fiber flexibility, fiber continuity and bonding ability jointly contribute to sheet deformability (Kouko et al. 2018; Ushakov et al. 2023).

Microstructural evolution of tobacco stems and tobacco stem-based sheets during refining

SEM and micro-CT were further used to visualize the microstructural evolution of tobacco stems and the corresponding sheet structures during multi-stage refining. As shown in Fig. 5a, the unrefined tobacco stem retained a compact and continuous tissue structure. The fiber bundles were tightly embedded in the matrix, and only limited fiber separation was observed. Such a compact structure restricts fiber swelling and inter-fiber bonding during sheet formation. After the first refining pass, the original tobacco stem tissue was partially opened, and the fiber bundles began to separate from the compact matrix (Fig. 5b). However, the fiber surface remained relatively smooth, indicating that one refining pass mainly promoted primary disintegration rather than sufficient fibrillation. After two refining passes, obvious fiber peeling, splitting and external fibrillation appeared on the fiber surface (Fig. 5c). This structure is favorable for increasing the contact area between fibers and improving inter-fiber bonding. When the refining pass increased to three, the fibers became more severely separated and fragmented (Fig. 5d). Although the fiber surface was further opened, excessive mechanical treatment could weaken the structural integrity of the coarse fiber skeleton.

The micro-CT cross-sectional images of the corresponding sheets further confirmed the structural transition during refining. The sheet prepared from unrefined tobacco stems showed a highly heterogeneous internal structure with obvious fiber aggregation and uneven density distribution (Fig. 5e). This indicates poor fiber dispersion and insufficient network formation. After one refining pass, the sheet became more uniform, but the internal fiber network was still relatively loose and discontinuous (Fig. 5f). After two refining passes, the sheet displayed a more homogeneous and interconnected fiber network (Fig. 5g), suggesting that moderate refining promoted fiber dispersion and bonding while maintaining sufficient internal pores. This structure is consistent with the maximum tensile strength and elongation obtained at 28 °SR. After three refining passes, the sheet structure became visibly denser (Fig. 5h). The increased amount of fibrillated and fine components filled the inter-fiber voids, leading to a more compact network (Mandlez et al. 2022). This explains the continuous decrease in bulk after refining, as well as the slight reduction in tensile strength and elongation at 31 °SR. Therefore, the microstructural observations demonstrate that two-stage refining is more favorable for forming a balanced hierarchical network, in which fibrillated fibers provide bonding strength while relatively intact coarse fibers maintain structural support and bulkiness.

Pore-network evolution of tobacco stem-based sheets revealed by micro-CT

Micro-CT analysis was used to further quantify the internal pore-network evolution of tobacco stem-based sheets prepared at different beating degrees. As shown in Fig. 6a, the sheet prepared at 22 °SR exhibited the lowest porosity among the refined samples, with a relatively fluctuating porosity profile along the XY slices. This indicates that one-pass refining was insufficient to fully disperse the tobacco

stem fibers, resulting in local fiber aggregation and heterogeneous pore distribution within the sheet. When the beating degree increased to 28 °SR, the overall porosity increased and the slice-by-slice porosity profile became more stable. This suggests that two-stage refining improves fiber separation and sheet formation uniformity. The enhanced fibrillation and better fiber dispersion allowed the formation of a more continuous porous network, while still preserving sufficient internal voids. This structural feature agrees well with the improved tensile strength and elongation observed at 28 °SR. At 31 °SR, the sheet also showed a relatively high porosity level; however, this did not lead to higher macroscopic bulk. This apparent difference can be explained by the refinement of pore structure. With further refining, more fibrillated fibers and fine components were generated, subdividing larger voids into smaller pores and compacting the overall fiber network. Therefore, the CT-derived porosity mainly reflects the total void fraction within the reconstructed region, whereas the macroscopic bulk is also affected by pore size, pore morphology, fiber packing and network compressibility (Reitbauer et al. 2023).

The pore size distributions further confirm this structural transition. The sheet prepared at 22 °SR showed a broad pore size distribution ranging approximately from 0.04 to 0.18 mm, with the main pore fraction centered around 0.08 mm (Fig. 6b). The relatively broad distribution indicates an uneven pore network caused by insufficient fiber dispersion. At 28 °SR, the pore size distribution became more concentrated in the medium pore range of approximately 0.06–0.10 mm, while the fraction of large pores decreased (Fig. 6c). This indicates that moderate refining promoted a more uniform pore network, which is beneficial for balancing sheet bulkiness and mechanical strength.

For the sheet prepared at 31 °SR, the pore size distribution became further concentrated around 0.06–0.08 mm, with a higher proportion of small and medium pores and fewer large pores (Fig. 6d). This demonstrates that excessive refining did not simply increase porosity but transformed the pore network from a loose structure with large voids into a finer and more compact porous architecture. Such pore refinement explains the continuous decrease in bulk from 12.212 to 10.155 $cm^3 \cdot g^{-1}$ as the refining pass increased, despite the relatively high CT porosity at higher beating degrees.

Conclusion

In this study, mild hot-water extraction combined with multi-stage refining was used to regulate tobacco stem fiber morphology and balance the bulkiness and strength of reconstituted tobacco sheets. Micro-CT showed that hot-water extraction loosened the compact internal structure of tobacco stems, facilitating subsequent fiber separation and fibrillation during refining.

Increasing the refining pass raised the beating degree from 22 °SR to 31 °SR and increased the fine pulp yield from 5.33% to 12.23%. Two-stage refining produced the most favorable fiber morphology, with sufficient fibrillation and limited fiber damage. Accordingly, the tensile strength and elongation reached their maximum values of 0.371 $kN \cdot m^{-1}$ and 1.030% at 28 °SR, while the sheet still maintained a relatively high bulk of 11.560 $cm^3 \cdot g^{-1}$. SEM and micro-CT analyses confirmed that insufficient refining led to poor fiber dispersion and heterogeneous pore structures, whereas excessive refining compacted the fiber

network and reduced bulk. Two-stage refining formed a more uniform and interconnected porous network, enabling the best balance between bulkiness and mechanical strength. This work provides a mild pretreatment and controlled refining strategy for the high-value utilization of tobacco stems in high-bulk reconstituted tobacco sheets.

Declarations

Competing Interests

The authors declare that they have no known competing financial interests or personal relationships that could have appeared to influence the work reported in this paper.

Funding

This work was supported by the State Key Laboratory of Pulp and Paper Engineering (Grant No. 2022ZD07).

Author Contribution

Qianqian Zhao: Conceptualization, Methodology, Investigation, Data curation, Visualization, Writing – original draft.Mengting Ye: Investigation, Data curation, Formal analysis, Visualization.Huilin Hu: Investigation, Methodology, Validation, Writing – review & editing.Xinke Yuan: Resources, Funding acquisition, Supervision, Project administration, Writing – review & editing.Jun Li: Conceptualization, Supervision, Project administration, Funding acquisition, Writing – review & editing.All authors reviewed the manuscript.

Data Availability

All data generated or analyzed during this study are included in the manuscript and its supplementary information files.All data generated or analyzed during this study are included in the manuscript and its supplementary information files.

References

1. Ang S, Haritos V, Batchelor W (2019) Effect of refining and homogenization on nanocellulose fiber development, sheet strength and energy consumption. Cellulose. https://doi.org/10.1007/s10570-019-02400-5
2. Berhanu Lemma H, Steffen F, Yimam Ali A, Saake B (2024) Production of Long-Fiber Pulp from Enset Plant Residues by Soda Pulping. Molecules. https://doi.org/10.3390/molecules29204874

3. Chaowei W, Henan Cigarette Industry Tobacco Sheet Ltd. XHC, Chong L, Fan X, Xiangfan W, Yangbing W (2019) Evaluation of the Potential of Tobacco Stalk Pulp to Substitute Hardwood Pulp for Tobacco Sheet Preparation. Cell Chem Technol 53:1009–1015
4. Dallé D, Hansen B, Zattera AJ, Francisquetti EL, Catto AL, Borsoi C (2021) Kinetic evaluation of tobacco stalk waste exposed to alkaline surface treatment under different conditions. Cellulose 28(4):2053–2073. https://doi.org/10.1007/s10570-020-03657-x
5. Hayase Y, Aonuma H, Takahara S, Sakaue T, Kaneko Si, Nakanishi H (2021) Fold analysis of crumpled sheets using microcomputed tomography. Phys Rev E. https://doi.org/10.1103/physreve.104.025005
6. He H, Chen L, Shi H, Gao Y, You X, Li C, Xing W, Liu X (2025) Kinetic analysis-informed design of thermally conductive heat-not-burn tobacco for applications. Ind Crop Prod. https://doi.org/10.1016/j.indcrop.2025.121969
7. Hu N, Liu X, Wei S, Yao J, Wang W, Liu B, Tang T, Jiang J, Wang L (2024) Current status and future prospects of pretreatment for tobacco stalk lignocellulose. Front Bioeng Biotechnol 12:1465419. https://doi.org/10.3389/fbioe.2024.1465419
8. Hu X, Sun J, Zhang F, Yang J, Wang R, Zhang Z, Guo Z, Zhou S, Wang Q, Song X (2025) Preparation and application of thermal conductive adhesive for reconstructed tobacco sheets with Al2O3. J Therm Anal Calorim. https://doi.org/10.1007/s10973-025-15113-8
9. Huang Z, Wang P, Zhang J, Zhang Y, Li D, Xu L, Lu L, Huang S-X, Zhou S, Liu H, Chen G, Tao J (2024) A Facile Method to Produce High-Bulk and High-Strength Rolled Reconstituted Tobacco Sheet with Refined Tobacco Cellulose Fibers. Cell Chem Technol
10. Huo P, Ma S, Li L, Liang W, Mo J, Zeng B, Nong H, Ding Z, Qian J, Li W, Zhou B (2023) Influence of tensile properties and fiber fraction on the mechanical properties of the sugarcane top anti-tangling in the silage industry. Ind Crop Prod. https://doi.org/10.1016/j.indcrop.2023.117898
11. Jamshaid H, Ahmad N, Hussain U, Mishra R (2022) Parametric optimization of durable sheeting fabric using Taguchi Grey Relational Analysis. Journal of King Saud University-Science. https://doi.org/10.1016/j.jksus.2022.102004
12. Kouko J, Jajcinovic M, Fischer W, Ketola A, Hirn U, Retulainen E (2018) Effect of mechanically induced micro deformations on extensibility and strength of individual softwood pulp fibers and sheets. Cellulose. https://doi.org/10.1007/s10570-018-2163-y
13. Kunfong N, Rattanawongkun P, Tawichai N, Intatha U, Soykeabkaew N (2023) The Influence of Refining on Molded Pulps from Banana Pseudostem Waste After NH4OH-KOH Based Pulping and Single-Stage Bleaching. Waste Biomass Valori. https://doi.org/10.1007/s12649-023-02253-x
14. Leszczyński M, Roman K (2023) Hot-Water Extraction (HWE) Method as Applied to Lignocellulosic Materials from Hemp Stalk. Energies. https://doi.org/10.3390/en16124750
15. Li J, Ye G, Wang J, Gong T, Wang J, Zeng D, Cifuentes A, Ibañez E, Zhao H, Lu W (2025) Recent advances in pressurized hot water extraction/modification of polysaccharides: Structure,

physicochemical properties, bioactivities, and applications. Compr Rev Food Sci F. https://doi.org/10.1111/1541-4337.70104

16. Li K-Y, Tang X-W, Zhao W-F, Fei M-L, Chen X-L, Liang J-X (2023) Microstructure characteristics of nonwoven geotextiles using SEM and CT methods. Geotext Geomembranes 51(2):293–302. https://doi.org/10.1016/j.geotexmem.2022.11.003
17. Li Y, Chen J, Yin S, Hu B, Lu H, Zeng W (2026) Reinforcement Learning Multi-Objective Optimization for the Refining Process of Reconstituted Tobacco Based on Pulp Fiber Morphology. In: 2026 7th International Seminar on Artificial Intelligence, Networking and Information Technology (AINIT), pp 402–406. https://doi.org/10.1109/AINIT70033.2026.11557731
18. Li Y, Chi Y, Han S, Zhao C, Miao Y (2021) Pore-throat structure characterization of carbon fiber reinforced resin matrix composites: Employing Micro-CT and Avizo technique. PLOS ONE. https://doi.org/10.1371/journal.pone.0257640
19. Li Y, Zhou H, Hu T, Shan S, Chen K, Zhao C, He L (2024) Mild three-stage alkali-oxygen treatment preserving the native macromolecular structure of lignin for effective disassembling of tobacco stalk. Int J Biol Macromol 279(Pt 4):135512. https://doi.org/10.1016/j.ijbiomac.2024.135512
20. Liu T, Wang Y, Wang C, Zhang Q, Wang L, Li Y, Xu L, Jin X, Yin X, Zhang Z, Luo C, Fu L, Wen Y, Li B (2024) Effect of plant fibers on the physical properties of slurry-processed reconstituted tobacco. Front Chem. https://doi.org/10.3389/fchem.2024.1463648
21. Liu Z, Xu X, Tang S, Si X, Liu C, Zhao H, Zhang F, Liu J, Ling Z, Zhu S (2026) Efficient extraction, compositional determination of tobacco stem via optimized hydrothermal treatment for efficient cellulose bioconversion. Sci Rep-UK. https://doi.org/10.1038/s41598-026-47078-5
22. Luo B, An X, Yang J, Liu L, Zhang H, Hu Q, Zhang R, Nie S, Wu S, Cao H, Cheng Z, Liu H (2021) Isolation and utilization of tobacco-based cellulose nanofiber (TCNF) for high performance reconstructed tobacco sheet (RTS). Carbohyd Polym. https://doi.org/10.1016/j.carbpol.2021.117865
23. Mandlez D, Koller S, Eckhart R, Kulachenko A, Bauer W, Hirn U (2022) Quantifying the contribution of fines production during refining to the resulting paper strength. Cellulose. https://doi.org/10.1007/s10570-022-04809-x
24. Motamedian HR, Halilovic AE, Kulachenko A (2019) Mechanisms of strength and stiffness improvement of paper after PFI refining with a focus on the effect of fines. Cellulose. https://doi.org/10.1007/s10570-019-02349-5
25. Puițel AC, Balan CD, Ailiesei G-L, Drăgoi EN, Nechita MT (2023) Integrated Hemicellulose Extraction and Papermaking Fiber Production from Agro-Waste Biomass. Polymers-Basel. https://doi.org/10.3390/polym15234597
26. Rech F, Pinto da Silva F, Roldo L, Duarte L (2023) Morphological, Chemical, and Thermal Characterization of Tobacco Stalk for Application in Composite Materials. Engineering And Technology Journal 8(5):2299–2305. https://doi.org/10.47191/etj/v8i5.15

27. Reitbauer J, Machado Charry E, Eckhart R, Sözeri C, Bauer W (2023) Bulk characterization of highly structured tissue paper based on 2D and 3D evaluation methods. Cellulose. https://doi.org/10.1007/s10570-023-05314-5
28. Samuel BO, Sumaila M, Dan-Asabe B (2022) Multi-objective optimization and modeling of a natural fiber hybrid reinforced composite (PxGyEz) for wind turbine blade development using grey relational analysis and regression analysis. Mech Adv Matl Struct. https://doi.org/10.1080/15376494.2022.2118404
29. Shakhes J, Marandi MAB, Zeinaly F, Saraian A, Saghaf T (2023) Tobacco residuals as promising lignocellulosic materials for pulp and paper industry. BioResources. https://doi.org/10.15376/biores.6.4.4481-4493
30. Sharma Y, Phillion AB, Martinez DM (2015) Automated segmentation of wood fibres in micro-CT images of paper. J Microsc-Oxford 260(3):400–10. https://doi.org/10.1111/jmi.12308
31. Song S, Wu Z, Tan J, Yang B, Zhang M, Lu P, Wang J, Li W (2021) Foam forming: an effective approach to fabricate highly bulky, uniform and soft reconstituted tobacco sheets. Cellulose. https://doi.org/10.1007/s10570-021-03677-1
32. Sood S, Sharma C (2021) Study on fiber furnishes and fiber morphological properties of commonly used Indian food packaging papers and paperboards. Cell Chem Technol 55:125–131. https://doi.org/10.35812/CelluloseChemTechnol.2021.55.13
33. Sun Q, Chen W-J, Pang B, Sun Z, Lam SS, Sonne C, Yuan T-Q (2021) Ultrastructural change in lignocellulosic biomass during hydrothermal pretreatment. BioResource Technol. https://doi.org/10.1016/j.biortech.2021.125807
34. Sung YJ, Seo YB (2009) Thermogravimetric study on stem biomass of Nicotiana tabacum. Thermochim Acta 486(1):1–4. https://doi.org/10.1016/j.tca.2008.12.010
35. Tao Y, Wang Z, Hadigheh SA (2025) Enhancing X-ray micro-CT analysis for detecting voids and carbon fibre features in fibre-reinforced cementitious composites using advanced 3D Gaussian filtering. Measurement 249. https://doi.org/10.1016/j.measurement.2025.117018
36. Ushakov A, Alashkevich Y, Pen R, Kozhukhov V (2023) Factor and cluster analyses of the structure of correlations between high consistency pulp properties during refining and paper strength characteristics. BioResources. https://doi.org/10.15376/biores.18.4.8090-8103
37. Vujji A, Dahiya R (2023) Enhancement of Weighting Coefficient Selection using Grey Relational Analysis for Model Predictive Torque Control of PMSM Drive: Analysis and Experiments. Distributed Generation & Alternative Energy Journal. https://doi.org/10.13052/dgaej2156-3306.3854
38. Wang Y, Liu Y, Chen J, Xu J, Shen W, Corriou J-P (2023) Multidirectional permeability simulation for fiber network based on the pore structure 3D characterization by CT scanning. Cellulose 31(1):187–203. https://doi.org/10.1007/s10570-023-05645-3
39. Zhao D, Deng Y, Han D, Tan L, Ding Y, Zhou Z, Xu H, Guo Y (2018) Exploring structural variations of hydrogen-bonding patterns in cellulose during mechanical pulp refining of tobacco stems. Carbohyd Polym. https://doi.org/10.1016/j.carbpol.2018.10.024

Figures

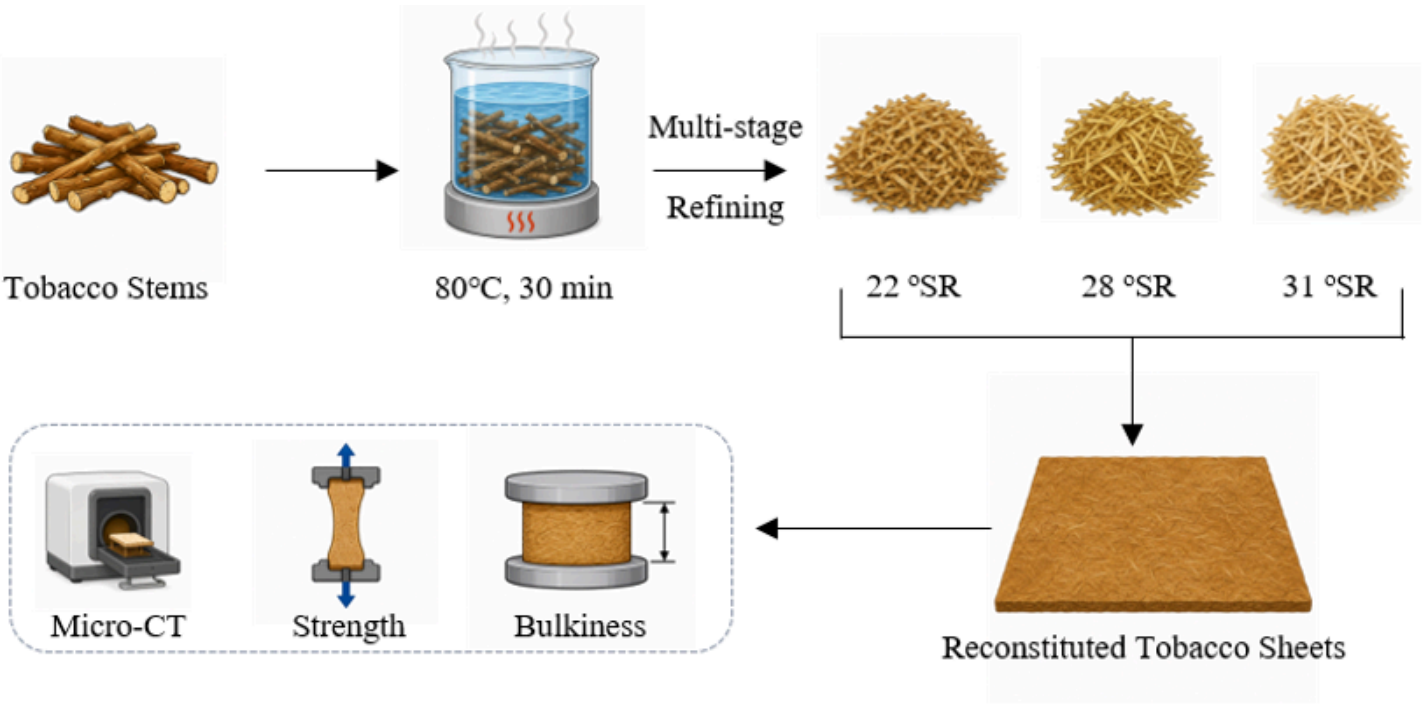


Figure 1

Schematic illustration of the preparation and characterization of reconstituted tobacco sheets from tobacco stems.

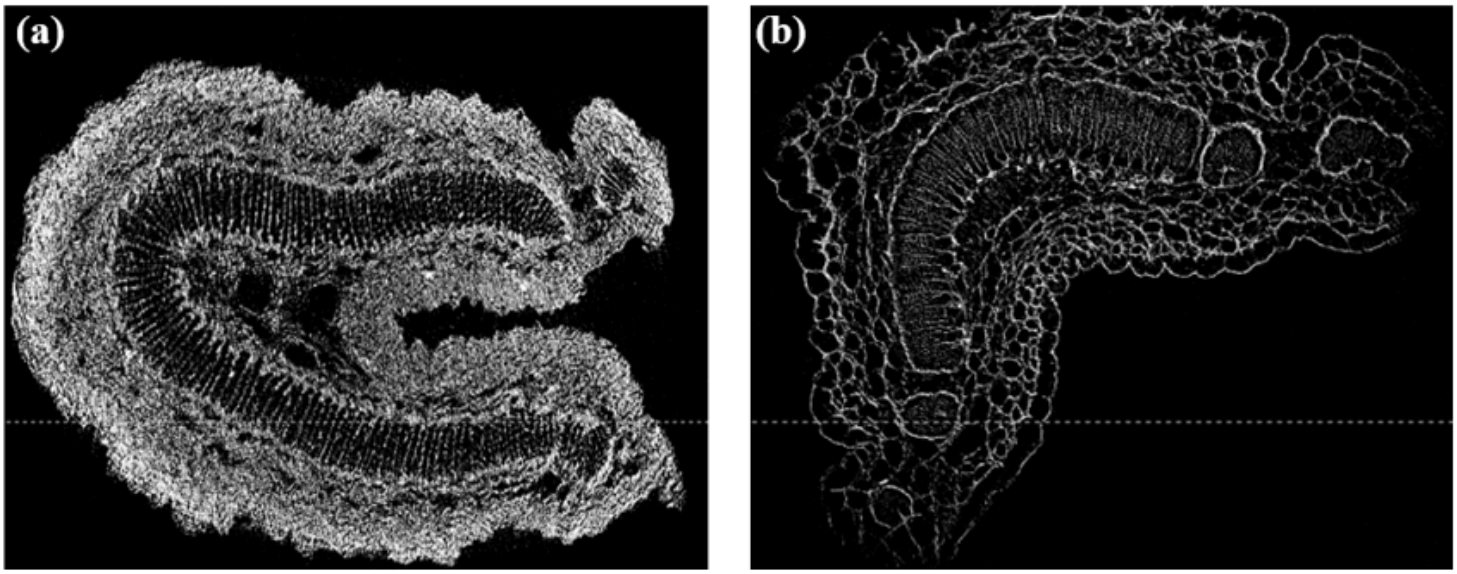


Figure 2

Micro-CT cross-sectional images of tobacco stems before and after hot-water extraction: (a) untreated tobacco stem and (b) hot-water-extracted tobacco stem.

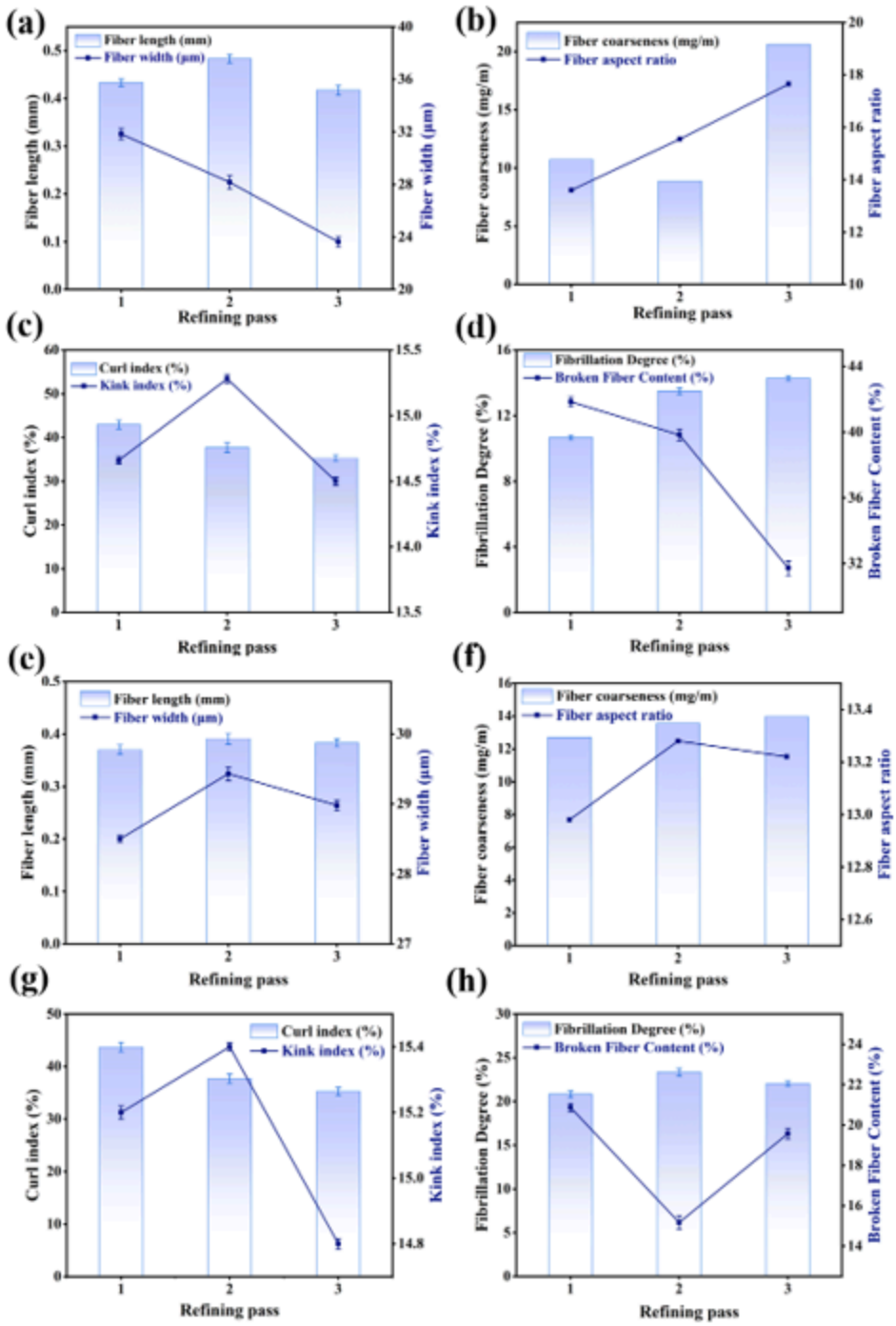


Figure 3

Changes in fiber morphology of coarse and fine pulp fractions during multi-stage refining. (a) Fiber length and fiber width of coarse pulp; (b) fiber coarseness and fiber aspect ratio of coarse pulp; (c) curl index and kink index of coarse pulp; (d) fibrillation degree and broken fiber content of coarse pulp; (e) fiber length and fiber width of fine pulp; (f) fiber coarseness and fiber aspect ratio of fine pulp; (g) curl index and kink index of fine pulp; (h) fibrillation degree and broken fiber content of fine pulp.

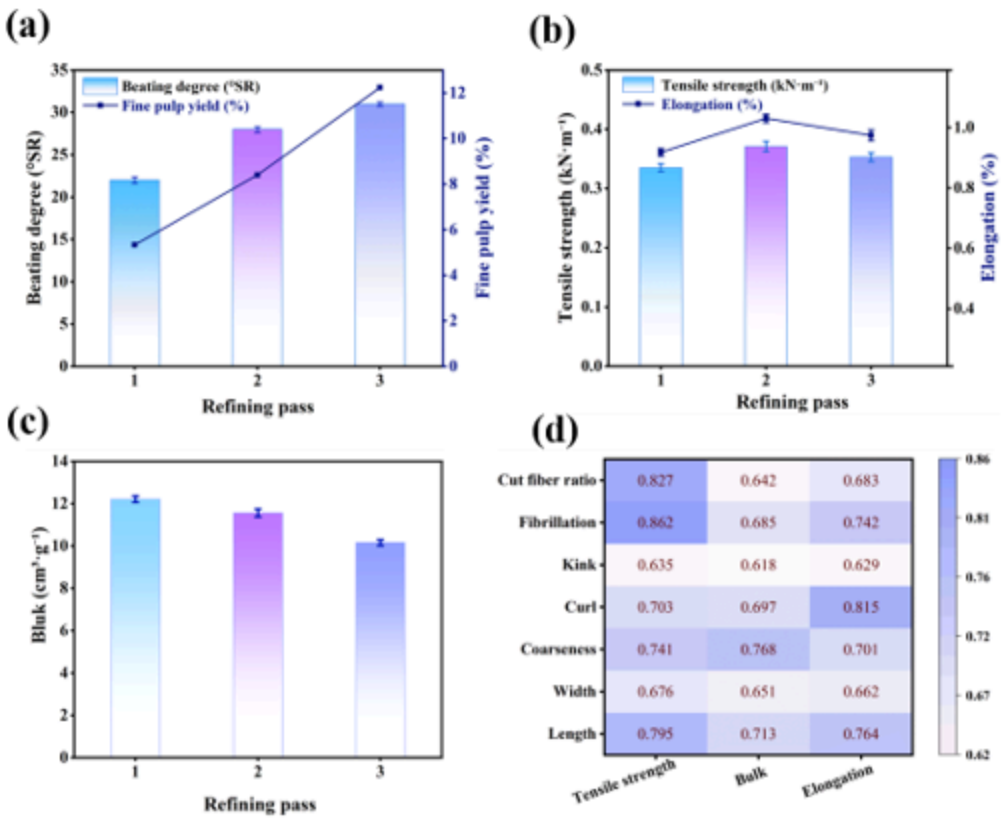


Figure 4

Effect of refining pass on pulp development, physical properties and fiber morphology-property relationships of reconstituted tobacco sheets. (a) Beating degree and fine pulp yield; (b) tensile strength and elongation; (c) bulk; (d) grey relational degree between fiber morphological characteristics and sheet properties.

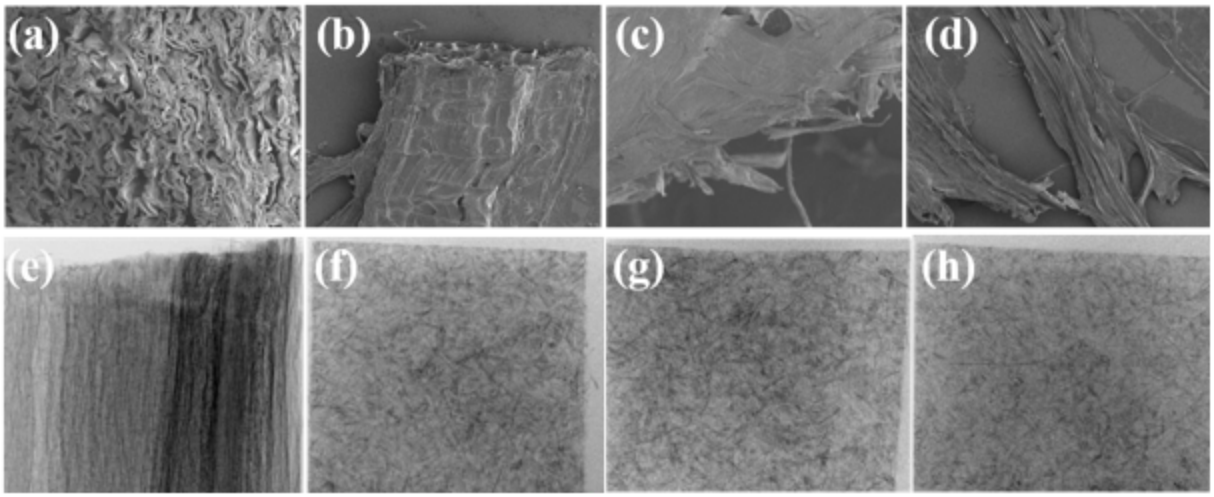


Figure 5

Microstructural evolution of tobacco stems and tobacco stem-based sheets during multi-stage refining. SEM images of tobacco stems: (a) unrefined tobacco stem; (b) tobacco stem after one refining pass; (c) tobacco stem after two refining passes; (d) tobacco stem after three refining passes. Micro-CT cross-sectional images of tobacco stem-based sheets: (e) sheet prepared from unrefined tobacco stem pulp; (f) sheet prepared from one-pass refined tobacco stem pulp,; (g) sheet prepared from two-pass refined tobacco stem pulp; (h) sheet prepared from three-pass refined tobacco stem pulp.

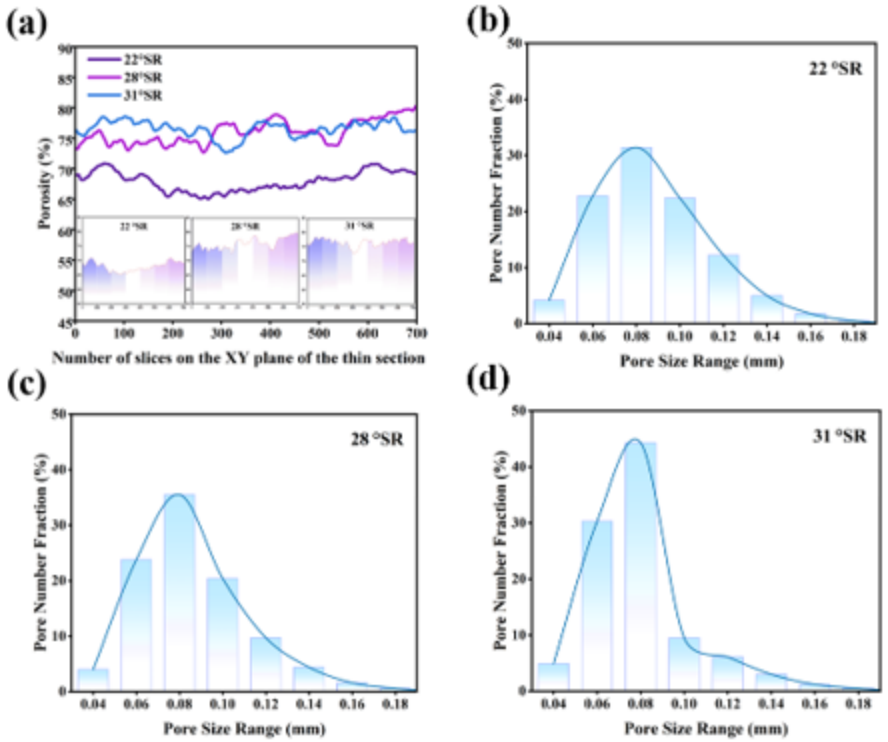


Figure 6

Micro-CT analysis of pore-network evolution in tobacco stem-based sheets prepared at different beating degrees. (a) Slice-by-slice porosity distribution of sheets prepared at 22 °SR, 28 °SR and 31 °SR along the XY plane; (b-d) pore size distributions of sheets prepared at 22 °SR, 28 °SR and 31 °SR.